

An *ab initio* investigation on the zinc-blende MnAs nanocrystallite

M. C. Qian, C. Y. Fong, and W. E. Pickett

Department of Physics, University of California, Davis, California 95616

Huai-Yu Wang

CCAST (World Laboratory), P.O. Box 8730, Beijing 100080, China and Department of Physics, Tsinghua University, Beijing 100084, China

(Presented on 9 January 2004)

Among a new class of spintronics materials, nanoscale dots of the zinc-blende (ZB) MnAs have recently been synthesized on the GaAs(001) surface. We apply an *ab initio* pseudopotential method with the generalized gradient approximation to study magnetic and structural stability for the Mn-centered ZB $\text{MnAs}_4\text{Mn}_{12}\text{As}_{24}$ cluster, which is relaxed both atomically and electronically. The ferromagnetic cluster is shown to have characteristics of a half metal with a large magnetic moment $4\mu_B$ per Mn atom. The Mn-As bond length is slightly longer than the one in the bulk, in accord with experimental observation. The “semiconducting” gap 1.83 eV is opened up in the minority channel, due to the large bonding-antibonding splitting from the *p-d* hybridization, similar to the ZB bulk MnAs and $\text{Ga}_{1-x}\text{Mn}_x\text{As}$. We also find an antiferromagnetic coupling in this system such that the moment of the central Mn atom is flipped with respect to those of the second-shell Mn atoms. © 2004 American Institute of Physics. [DOI: 10.1063/1.1687291]

Since the first success in growing epitaxial films of CrAs with zinc-blende (ZB) structure on the GaAs substrate,¹ much attention has been paid to this new class of material, i.e., the ZB half-metal (HM) where electrons with spins polarized in one direction exhibit metallic behaviors and spins polarized in the opposite direction show semiconducting properties. Many groups around the world have vigorously investigated these zinc-blende (ZB) compounds of transition metals theoretically and experimentally,^{1–6} which will be excellent candidates for the spintronic applications in the future, because they have 100% spin polarization at the Fermi energy, large magnetic moment, high Curie temperature T_c (around room temperature), and coherent growth on semiconductor substrate.

Recently, Ono *et al.*⁷ have grown nanoscale dots of ferromagnetic MnAs on a sulfur-passivated GaAs(001) surface under As-rich condition by molecular-beam epitaxy and observed the remnant magnetization with $T_c \approx 280$ K. They used transmission electron microscopy and selected area electron diffraction to confirm that the crystalline structure of MnAs was the zinc-blende type. Their photoemission spectroscopic experiments show that the Mn *3d* partial density of states in the ZB MnAs dots was similar to that of diluted ferromagnetic semiconductor $\text{Ga}_{1-x}\text{Mn}_x\text{As}$. From a theoretical viewpoint, it is very important to understand the electronic and magnetic properties of such nanoscale ZB MnAs dots. In this paper, we discuss in detail the electronic structures of the ZB MnAs nanocrystallite using the example of $\text{MnAs}_4\text{Mn}_{12}\text{As}_{24}$ cluster under ferromagnetic (FM) and antiferromagnetic (AFM) orders.

First-principles total energy and electronic structure calculations have been performed using the pseudopotential plane-wave method based on density functional theory⁸ (DFT) within the generalized gradient approximation (GGA).⁹ We used the VASP program^{10,11} for our spin polar-

ized calculations in which ultrasoft pseudopotentials¹² are used for Mn and As atoms with normal valence electron configurations. The cutoff energy is taken to be 300 eV. In order to simulate the isolated cluster, we use a large face-centered cubic (fcc) supercell whose size is four times the equilibrium lattice constant of bulk ZB MnAs, i.e., 22.96 Å. Brillouin zone integrations have been done on only the Γ point due to the isolated quantum dots, using a Gaussian smearing of $\sigma = 0.2$ eV. All atoms are allowed to relax and the equilibrium positions are identified when the forces are smaller than 0.05 eV/Å.

The model MnAs dot containing 41 atoms was constructed using the zinc-blende crystal structure up to a cutoff radius of 6.1 Å. Such a $\text{MnAs}_4\text{Mn}_{12}\text{As}_{24}$ cluster is shown in Fig. 1, which has one central Mn atom, four neighboring As atoms, 12 second-shell Mn atoms, and 24 third-shell As at-

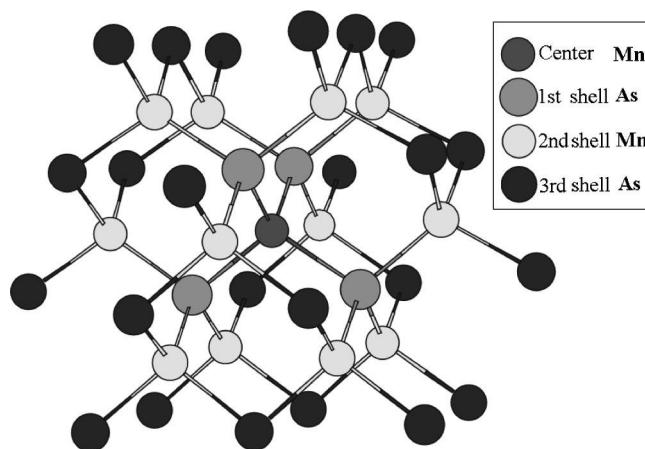


FIG. 1. A model of the zinc-blende MnAs quantum dot by the $\text{MnAs}_4\text{Mn}_{12}\text{As}_{24}$ cluster. The third As shell is saturated by pseudohydrogens.

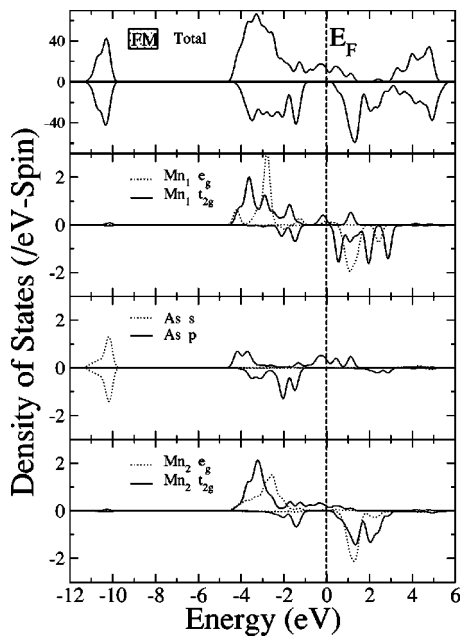


FIG. 2. Total and projected densities of states for the ferromagnetic $\text{MnAs}_4\text{Mn}_{12}\text{As}_{24}$ cluster. Mn_1 and Mn_2 are referred to as the center and the second-shell manganese, respectively. The positive (negative) values represent the majority (minority) spin channel. The Fermi level is set to zero. The DOS's have been broadened by the Gaussian smearing with 0.2 eV.

oms. We put this cluster at the lattice points of fcc supercell with the size of 22.96 Å, which make the nearest distance between atoms in neighboring clusters to be 4.06 Å. In order to passivate the dangling bonds on the cluster surface, we use 60 pseudohydrogens with an effective atomic number of 0.75 to saturate 24 third-shell As atoms. Starting from the ideal ionic positions in the bulk ZB MnAs, we can get the stable geometric structures in both ferromagnetic and antiferromagnetic phases. The average bond length of the center MnAs_4 slightly increases to 2.491 Å for FM phase, but compresses to 2.470 Å for AFM phase, compared to the bond length 2.486 Å of bulk ZB MnAs (Ref. 6) at the equilibrium lattice constant 5.74 Å. It can be understood that the AFM alignment always prefers some contraction, due to the exchange striction.¹³

In Fig. 2, we show the total and projected densities of states (DOS's) for the $\text{MnAs}_4\text{Mn}_{12}\text{As}_{24}$ cluster in the ferromagnetic phase. The total magnetic moment of $52\mu_B$ is obtained. The cluster presents half-metallic character with a gap of 1.83 eV in the minority spin DOS near E_F , but without any gap in the majority spin channel. The metallic majority spin DOS at E_F is composed largely of As p states and Mn t_{2g} states, suggesting that the hybridization between As p –Mn t_{2g} is responsible for the half metallicity. The states at about -10 eV have As s character and are energetically isolated from the bonding states. The orbital resolved DOS for the $3d$ states is different for the central and the second-shell manganese atoms. Considering the majority spin, the central Mn_1 t_{2g} states are split into three peaks over the range from -1.0 eV to -4.0 eV, which reflects the small distortion of the tetrahedral structure of MnAs_4 at the center of the cluster. The Mn_1 e_g states characterized by a strong peak at -2.9 eV are fully occupied and have a non-

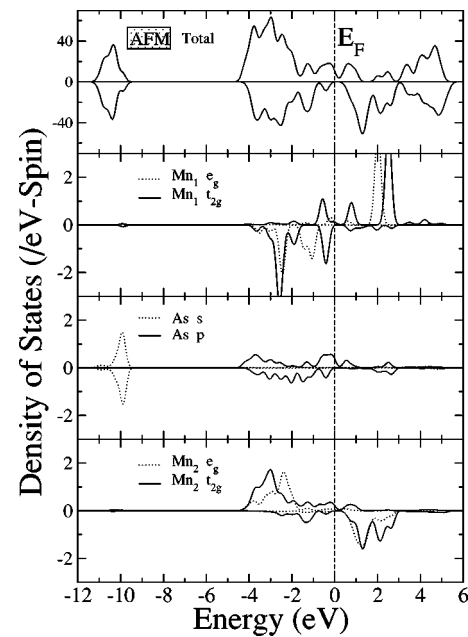


FIG. 3. Total and projected densities of states for the antiferromagnetic $\text{MnAs}_4\text{Mn}_{12}\text{As}_{24}$ cluster. Mn_1 and Mn_2 are referred to as the center and the second-shell manganese, respectively. The positive (negative) values represent the majority (minority) spin channel. The Fermi level is set to zero. The DOS's have been broadened by the Gaussian smearing with 0.2 eV.

bonding character. The distribution of the partial DOS for the second-shell Mn_2 is quite similar to that of ZB bulk MnAs and $\text{Ga}_{1-x}\text{Mn}_x\text{As}$, which is consistent with experimental observation.⁷ The Mn_2 t_{2g} states lie at -3.7 eV and e_g states at -2.4 eV. For the minority spin channel, the d states are shifted about 3 eV relative to the majority by the exchange interaction. The peak at -1.7 eV is from the bonding p – d hybrids with the dominant As p character than the d states features of the Mn atom. The gap separates the bonding and nonbonding states.

We also give the total and projected densities of states for the antiferromagnetic $\text{MnAs}_4\text{Mn}_{12}\text{As}_{24}$ cluster in Fig. 3. We find that some half-metallic tendency is still preserved with a small gap of 0.97 eV in the minority spin channel. Because of the competition between FM double exchange and AFM superexchange interactions in the system, the formal configuration of the central Mn_1 after flipping of the spin becomes d^5 , which further stabilizes the AFM superexchange coupling, while the excess electron comes from the second-shell Mn_2 . The total magnetic moment $13 \times 4\mu_B$ for FM order is reduced to $(12 \times 4 - 1) - 5 = 42\mu_B$ for AFM alignment. Energetically, this AFM order is more stable than the FM phase by an energy of 125 meV. From Fig. 3, it can be seen that the central Mn_1 becomes electronically “separated” from the second-shell Mn_2 . The local structure around the central Mn_1 atom is somewhat distorted, resulting in the splitting of Mn_1 d states. Comparing to the FM case, the distribution of As p states is shifted and broadened. The second-shell Mn_2 is almost unaffected by the flipping of magnetic moment in the central Mn_1 atom.

In summary, we have investigated the zinc-blende MnAs nanocrystallite using an *ab initio* pseudopotential method with a plane-wave basis. Using an example of the

MnAs₄Mn₁₂As₂₄ cluster, we found that the ZB MnAs dots show half-metallic character in both ferromagnetic and anti-ferromagnetic (central Mn spin reversal) phases. In the FM case, each Mn atom contributes a magnetic moment of $4\mu_B$. The semiconducting gap in the minority spin channel is 1.83 eV, which is slightly larger than that of bulk ZB MnAs. When we flip the magnetic moment of central Mn atom, the cluster is more stable by 125 meV. However, the gap is reduced to 0.97 eV and the total magnetic moment $42\mu_B$, as if a central spin of $5\mu_B$ had flipped. We suggest that such FM ZB MnAs dots are metastable and could be stabilized on the GaAs(001) surface.

The work at UC Davis was supported in part by NSF grants with Grants Nos. ESC-0255007 and INT-9872053, Materials Research Institute at Lawrence Livermore National Laboratory (LLNL), NERSC at Lawrence Berkeley National Laboratory, and the Research Committee at UC Davis.

- ¹H. Akinaga, T. Manago, and M. Shirai, *Jpn. J. Appl. Phys.*, Part 2 **39**, L1118 (2000).
- ²J. H. Zhao, F. Matsukura, T. Takamura, E. Abe, D. Chiba, and H. Ohno, *Appl. Phys. Lett.* **79**, 2776 (2001).
- ³S. Sanvito and N. A. Hill, *Phys. Rev. B* **62**, 15553 (2000).
- ⁴Y.-J. Zhao, W. T. Geng, A. J. Freeman, and B. Delley, *Phys. Rev. B* **65**, 113202 (2002).
- ⁵I. Galanakis and P. Mavropoulos, *Phys. Rev. B* **67**, 104417 (2003).
- ⁶J. E. Pask, L. H. Yang, C. Y. Fong, W. E. Pickett, and S. Dag, *Phys. Rev. B* **67**, 224420 (2003).
- ⁷K. Ono, J. Okabayashi, M. Mizuguchi, M. Oshima, A. Fujimori, and H. Akinaga, *J. Appl. Phys.* **91**, 8088 (2002).
- ⁸P. Hohenberg and W. Kohn, *Phys. Rev.* **136**, B864 (1964); W. Kohn and L. J. Sham, *Phys. Rev.* **140**, A1133 (1965).
- ⁹J. P. Perdew, K. Burke, and M. Ernzerhof, *Phys. Rev. Lett.* **77**, 3865 (1996); J. P. Perdew and Y. Wang, *Phys. Rev. B* **45**, 13244 (1992).
- ¹⁰VASP, Institut für Theoretische Physik of the Technische Universität, Wien, Austria.
- ¹¹G. Kresse and J. Hafner, *J. Phys.: Condens. Matter* **6**, 8245 (1994); G. Kresse and J. Furthmüller *Phys. Rev. B* **54**, 11169 (1996).
- ¹²D. Vanderbilt, *Phys. Rev. B* **41**, 7892 (1990).
- ¹³I. V. Solovyev and K. Terakura, in *Electronic Structure and Magnetism of Complex Materials*, edited by D. J. Singh and D. A. Papaconstantopoulos (Springer, Berlin, 2003), p. 253.